Phase Transitions

# Direct Observation of Bonding and Charge Ordering in $(EDO\text{-}TTF)_2PF_6$**

*Shinobu Aoyagi, Kenichi Kato, Akira Ota, Hideki Yamochi, Gunzi Saito, Hiroyoshi Suematsu, Makoto Sakata, and Masaki Takata**

The characteristics of the metal–insulator (MI) phase transition in $[(EDO\text{-}TTF)(EDO\text{-}TTF^{+})PF_6^{-}]$ (EDO-TTF = ethylenedioxytetrathiafulvalene) have been suggested so far to be the result of cooperative phenomena: Peierls distortion, charge ordering, anion ordering, and the molecular deformation which is evident from the single-crystal X-ray analysis and the peak shifts in the Raman spectrum.[1,2] However, there has been no direct evidence of charge-ordering patterns connected with the MI transition. Herein, we present direct evidence for an ordering of $(EDO\text{-}TTF)^{+}$ and $(EDO\text{-}TTF)^{0}$ along the nesting vector visualized in the $(EDO\text{-}TTF)_2PF_6$ charge density distributions obtained by a combination of the MEM (maximum entropy method) and the Rietveld method.[3–9] The charge transfer and coulombic interactions between $PF_6^{-}$ anions and EDO-TTF molecules as well as a hole concentration on one S atom in $(EDO\text{-}TTF)^{+}$ were also revealed by the charge densities. In addition, a bonding between the EDO-TTF molecules that suggests quasi-one-dimensional (1D) properties was found in the MEM charge density. Changes in the bonding during the MI transition that may explain the existence of the insulator singlet state also became evident.

A number of 1D organic conductors that are formed from large planar electron-donating molecules such as TTF derivatives have been studied extensively because of their attractive phase transitions and the possibility of using them in functional molecular devices.[10,11] Most of the MI transitions can be classified as Peierls transitions, charge ordering, Mott transitions, or Anderson localization.[10–15] The MI transition in the $^3/_4$-filled-band ($^1/_4$-filled in terms of holes) quasi-1D system $(EDO\text{-}TTF)_2PF_6$ ($C_{16}H_{12}S_8O_4PF_6$) ($T_{MI} \approx 280$ K), however, has been considered as the particular example which shows the cooperative action of Peierls distortion, charge ordering, and anion ordering, together with a molecular deformation.[1,2] The charge-ordering pattern of EDO-TTF donor molecules has been suggested to be [0,0,+1,+1,…] by previous studies,[1,2] despite the fact that in most $^1/_4$-filled-band 1D systems the ordering pattern [0,+1,0,+1,…] is found as a result of strong neighbor-site coulombic interactions.[13–15] Recently, ultrafast photoswitching from the insulator to the metallic phase has also been reported for this system.[16] The peculiar phase transition in $(EDO\text{-}TTF)_2PF_6$ is quite attractive for a better understanding of cooperative and coherent phenomena in organic conductors. However, the structural information was limited to the atomic parameters when conventional single-crystal X-ray analysis was applied.[1] More detailed information on the MI transition, such as intermolecular bonding and charge transfer between molecules, must be obtained by an X-ray charge-density study.[17–19]

The synchrotron-radiation (SR) powder-diffraction experiment with imaging-plate (IP) detectors was carried out with the large Debye–Scherrer camera at SPring-8 BL02B2.[20] The wavelength of the incident X-rays was 1.0 Å. Data were measured for the metallic phase at 285 K and for the insulator phase at 260 K and analyzed by the MEM/Rietveld method.[3,21,22] This method has been successfully applied, for example, in charge-density studies of fullerene compounds,[3–6] intermetallic compounds,[7] α-boron,[8] and manganite.[3,9] In the case of metallofullerenes, it has revealed charge transfer from the encapsulated metal atom to the fullerene cage.[3–6] The best-fit plots of the results of the Rietveld analyses are shown in Figure 1. The reliability

[*] K. Kato, Prof. Dr. H. Suematsu, Prof. Dr. M. Takata
SPring-8/JASRI
Kouto, Mikazuki, Sayo, Hyogo 679-5198 (Japan)
Fax: (+81) 791-58-0946
E-mail: takatama@spring8.or.jp
Dr. S. Aoyagi, Prof. Dr. M. Sakata
Department of Applied Physics
Nagoya University
Nagoya 464-8603 (Japan)
A. Ota, Prof. Dr. G. Saito
Division of Chemistry
Graduate School of Science
Kyoto University
Sakyo-ku, Kyoto 606-8502 (Japan)
Prof. Dr. H. Yamochi
Research Center for Low Temperature and Materials Sciences
Kyoto University
Sakyo-ku, Kyoto 606-8502 (Japan)

[**] We thank Dr. E. Nishibori for his help in the MEM/Rietveld analyses. The synchrotron radiation experiments were performed at SPring-8 BL02B2 with the approval of the Japan Synchrotron Radiation Research Institute (JASRI). This work was partly supported by Grants-in-Aid for scientific research and for the 21st century COE program of Kyoto University Alliance for Chemistry from the Ministry of Education, Culture, Sports, Science and Technology of Japan. This work was also supported by the Showa Shell Environmental Research Foundation.

  DOI: 10.1002/ange.200454075 

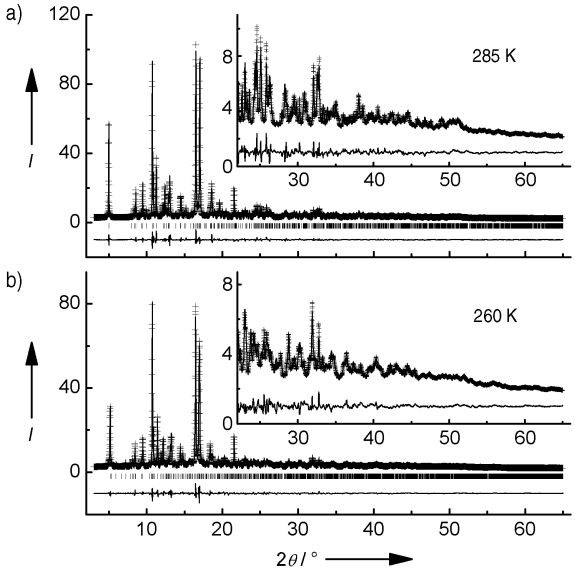


***Figure 1.*** Best-fit plots of the results of Rietveld analysis for metallic (a) and insulating (b) $(EDO\text{-}TTF)_2PF_6$. The data up to 65° in $2\theta$, which corresponds to 0.93 Å in $d$ spacing, were used in the analyses. The high-angular region is shown enlarged in the insets.

factors based on the Bragg intensities, $R_I$, and on the weighted profile, $R_{WP}$, were 0.0375 (0.0338) and 0.0447 (0.0425), respectively, for the metallic (insulator) phase. A total of 1564 (3093) independent structure factors were used in the MEM analyses, which were carried out with the unit cell divided into $64 \times 64 \times 128$ ($128 \times 128 \times 128$) pixels by using the program ENIGMA.[23] The $R$ factor based on the structure factors, $R_{MEM}$, for the final MEM charge densities was 0.0285 (0.0528).

The equi-charge-density surfaces at the level of 0.7 e Å$^{-3}$ of metallic and insulating $(EDO\text{-}TTF)_2PF_6$ are shown in Figure 2. In both the metallic and the insulator phases, layers of EDO-TTF molecules form columns by a head-to-tail stacking perpendicular to the molecular plane, which provides a donor layer parallel to the $ab$ plane. $PF_6^-$ anions are located at the cavities between the EDO-TTF layers. Whereas the metallic and insulator phases have the same space group $P\bar{1}$, the unit cell is doubled in the insulator phase ($Z = 2$), corresponding to a Peierls instability along the [110] direction in the cell of the metallic phase ($Z = 1$). Cell parameters were derived as $a_M = 7.1942$, $b_M = 7.3214$, $c_M = 11.9304$ Å, $\alpha_M = 93.345$, $\beta_M = 75.054$, $\gamma_M = 97.435°$ for the metallic phase, and $a_I = 10.9898$, $b_I = 9.7954$, $c_I = 11.4864$ Å, $\alpha_I = 80.734$, $\beta_I = 78.079$, $\gamma_I = 90.241°$ for the insulator phase. The averaged intermolecular distances in the insulator phase are 0.7 and 2.3 % longer along $a$ and $b$ and 3.7 % shorter along $c$ than those in the metallic phase.

The $PF_6^-$ anions are disordered in the metallic phase (overlapping of two octahedra with a tilt of about 50°), whereas they are ordered in the insulator phase. These results are slightly different from the results of reference [1], and indicate an isotropic-to-uniaxial rotational ordering of the $PF_6^-$ anions. The reason for this discrepancy may be the poor quality of the previous diffraction data. In the insulator phase, two types of EDO-TTF molecules are present, flat and bent molecules, whereas in the metallic phase, there is only one type of EDO-TTF molecule. This molecular-shape change associated with the MI transition is in good agreement with the previously reported X-ray structure model.[1]

Since MEM charge densities reflect total electron densities, the charge states of EDO-TTF and $PF_6^-$ can be examined by counting the number of electrons around them, as was done in the metallofullerene studies.[3–6] The results for the metallic phase (Figure 2a,c) are $+0.6(1)$ e for EDO-TTF and $-1.2(1)$ e for $PF_6^-$. For the insulator phase (Figure 2b,d), the results are $+0.8(1)$ e for flat EDO-TTF, $+0.2(1)$ e for bent EDO-TTF, and $-1.0(1)$ e for $PF_6^-$. Thus, the bent EDO-TTF molecules are almost electrically neutral and the flat EDO-TTF molecules have an excess charge concentration close to $+1$ e in the insulator phase. This is the first direct evidence of a charge-ordering pattern.

The $PF_6^-$ anions are located close to the sulfur atoms S1 (S11, S21) and S4 (S14, S24), and to the terminal hydrogen atoms of the EDO-TTF molecules (see Figure 2). The distances between the $PF_6^-$ anions and the neighboring sulfur atoms are given in Figure 3 for both phases. The MI transition leads not only to a rotational ordering of the $PF_6^-$ anions but also to their displacement from the inversion center by 0.26 Å. This has the biggest effect on the P–S11 distance, which is shortened from 4.32 to 4.14 Å. A particular electrostatic interaction between $PF_6^-$ and S11 must play an important role in this shortening. To investigate the local charge concentration, the charge-density differences, $\Delta\rho$,

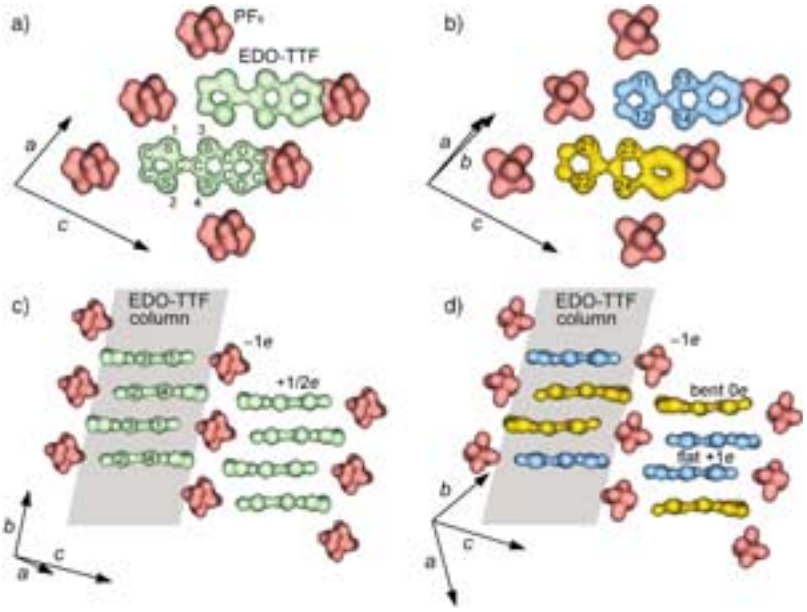


***Figure 2.*** Equi-charge-density surfaces of metallic ((a) and (c)) and insulating ((b) and (d)) $(EDO\text{-}TTF)_2PF_6$ at the level of 0.7 e Å$^{-3}$. The views in (a) and (b) are along the EDO-TTF stacking direction; in (c) and (d), side views of the EDO-TTF columns are shown. The $PF_6^-$ anion is colored in red. The EDO-TTF molecules are colored in green for the metallic phase, and in blue and yellow for the flat and bent molecules, respectively, for the insulator phase. Sulfur atoms are labeled S1–S4 for the metallic phase and S11–S14, S21–S24 for the insulator phase.

  

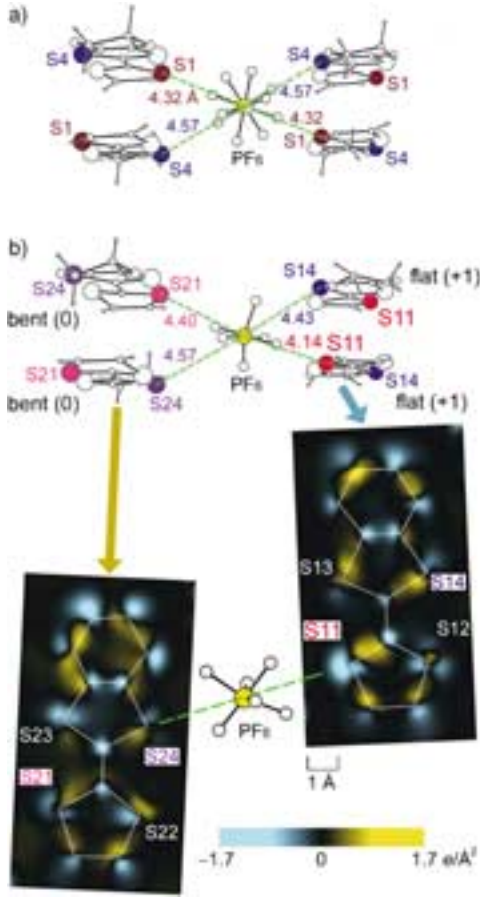


***Figure 3.*** Structure model and interatomic distances between P and S atoms for the metallic phase (a) and for the insulator phase (b). The charge-density differences for the bent and flat EDO-TTF molecules in the insulator phase, integrated perpendicular to the molecular plane for the range of ±1.5 Å, are also shown in (b); blue: residual positive charge; yellow: residual negative charge.

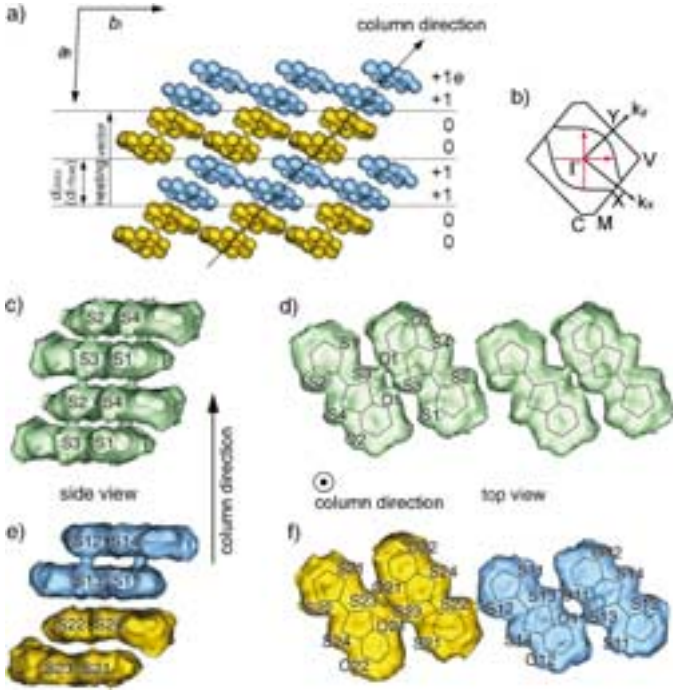


***Figure 4.*** MEM equi-charge-density surface of an EDO-TTF layer at 0.7 e Å$^{-3}$ and charge-ordering pattern in the insulator phase viewed along the *c* axis (a). Schematic Fermi surface in the $a^*b^*$ plane for the metallic phase, with red arrows indicating the $2k_F$ nesting vectors (b). Side and top views of the lower MEM equi-charge-density surfaces of EDO-TTF columns in the metallic phase ((c) and (d)) and in the insulator phase ((e) and (f)). The levels of the surfaces are 0.11 for (c) and (d) and 0.13 e Å$^{-3}$ for (e) and (f).

between the observed MEM charge density, $\rho_{obs}$, and the density calculated based on an arrangement of neutral free atoms, $\rho_{cal}$, for the bent and flat EDO-TTF molecules in the insulator phase are also shown in Figure 3b. As can be seen from Figure 3b, there is a significant positive-charge concentration around the S11 atomic site in flat EDO-TTF compared to the corresponding S21 site in bent EDO-TTF, which indicates that the conduction holes of the metallic phase are localized and trapped on the S11 atoms of the flat molecules in the insulator phase. Therefore, the local electrostatic P–S11 interaction should contribute to the hole trapping on the S11 atom. In addition, it is plausible that the suppression of the anion rotation is caused by the anion displacement that is necessary to increase the electrostatic stabilization.

The hole trapping on the EDO-TTF molecule and the displacement of the $PF_6^-$ anion alternate in the *ab* plane with a periodicity of $2k_F$ ($2\boldsymbol{k}_F = (\boldsymbol{a}^*_M \pm \boldsymbol{b}^*_M)/2$: nesting vector of the Fermi surface). As a result, the [0,0,+1,+1,…] ordering of the charges is along the $a^*_I$ axis ($[1\bar{1}0]_M$, Figure 4a), whereas a [0,+1,0,+1,..] ordering is expected for a $^1/_4$-filled-band system if there is no Peierls instability and if off-site Coulomb repulsions are effective.[13–15]

The side view of the lower equi-charge-density surface of an EDO-TTF column in the metallic phase at 0.11 e Å$^{-3}$ (Figure 4c) reveals intracolumnar intermolecular overlap of charge density, thus indicating a weakly bonded S2···S3···S2···S3··· chain. This chain is considered as a 1D conducting path of holes along the EDO-TTF stacking axis. Figure 4d shows a top view of the EDO-TTF columns. In the intercolumnar region, charge-density overlap occurs between S3 and O1 atoms. It has been argued that the contribution of the external oxygen atoms to the highest occupied molecular orbital (HOMO) in BEDO-TTF complexes is less than that of the internal sulfur atoms.[24] However, it is suggested that the external O1 atoms in $(EDO\text{-}TTF)_2PF_6$ participate greatly in the intercolumnar interaction to increase the electronic dimensionality of the complex.

The lower equi-charge-density surfaces of EDO-TTF columns in the insulator phase at 0.13 e Å$^{-3}$ are shown in Figure 4e,f. The charge-density overlaps between EDO-TTF columns in the insulator phase and in the metallic phase are very similar (Figure 4d,f). On the other hand, there is a significant change in the intracolumnar intermolecular charge density accompanying the MI transition (see Figure 4c,e). The bond between the flat molecules still exists, whereas the bonds between flat and bent molecules and between bent

  

molecules vanish. In other words, the flat $(EDO\text{-}TTF)^+$ molecules in the insulator phase are dimerized to provide a singlet state, consistent with the diamagnetism observed.[1] From the viewpoint of the intermolecular orbital interactions, this dimerization stabilizes the electronic structure overcoming the neighbor-site Coulomb repulsion and thus causing the [0,0,+1,+1,…] charge-ordering pattern.

In conclusion, our study revealed that the molecular displacements observed in the metal–insulator phase transition of $(EDO\text{-}TTF)_2PF_6$ assist the anion ordering and the electrostatic and electronic stabilization of the crystal structure of the insulator phase. The cooperativity in this peculiar MI transition shall be regarded as a result of the molecular displacement that occurs along the nesting vector in the metallic phase. Along with the bistability illustrated by the thermal hysteresis of this transition, the cooperativity should contribute to our understanding of the origin of this ultrafast photo-induced phase transition.

Received: February 23, 2004 [Z54075]

**Keywords:** charge density · organic conductors · synchrotron radiation · tetrathiafulvalenes · X-ray diffraction

[1] A. Ota, H. Yamochi, G. Saito, *J. Mater. Chem.* **2002**, *12*, 2600 – 2602.
[2] O. Drozdova, K. Yakushi, A. Ota, H. Yamochi, G. Saito, *Synth. Met.* **2003**, *133–134*, 277 – 279.
[3] M. Takata, E. Nishibori, M. Sakata, *Z. Kristallogr.* **2001**, *216*, 71 – 86.
[4] E. Nishibori, M. Takata, M. Sakata, A. Taninaka, H. Shinohara, *Angew. Chem.* **2001**, *113*, 3086 – 3087; *Angew. Chem. Int. Ed.* **2001**, *40*, 2998 – 2999.
[5] C. R. Wang, T. Kai, T. Tomiyama, T. Yoshida, Y. Kobayashi, E. Nishibori, M. Takata, M. Sakata, H. Shinohara, *Nature* **2000**, *408*, 426 – 427.
[6] M. Takata, B. Umeda, E. Nishibori, M. Sakata, Y. Saito, M. Ohno, H. Shinohara, *Nature* **1995**, *377*, 46 – 49.
[7] Y. Kubota, M. Takata, M. Sakata, T. Ohba, K. Kifune, T. Tadaki, *J. Phys. Condens. Matter* **2000**, *12*, 1253 – 1259.
[8] M. Fujimori, T. Nakata, T. Nakayama, E. Nishibori, K. Kimura, M. Takata, M. Sakata, *Phys. Rev. Lett.* **1999**, *82*, 4452 – 4455.
[9] M. Takata, E. Nishibori, K. Kato, M. Sakata, Y. Moritomo, *J. Phys. Soc. Jpn.* **1999**, *68*, 2190 – 2193.
[10] T. Ishiguro, K. Yamaji, G. Saito, *Organic Superconductors*, Springer, New York, **1998**.
[11] N. F. Mott, *Metal–Insulator Transitions*, Taylor&Francis, London, **1990**.
[12] H. Seo, *J. Phys. Soc. Jpn.* **2000**, *69*, 805 – 820.
[13] K. Hiraki, K. Kanoda, *Phys. Rev. Lett.* **1998**, *80*, 4737 – 4740.
[14] D. S. Chow, F. Zamborszky, B. Alavi, D. J. Tantillo, A. Baur, C. A. Merlic, S. E. Brown, *Phys. Rev. Lett.* **2000**, *85*, 1698 – 1701.
[15] P. Monceau, F. Ya. Nad, S. Brasovskii, *Phys. Rev. Lett.* **2001**, *86*, 4080 – 4083.
[16] N. Uchida, S. Koshihara, T. Ishikawa, A. Ota, S. Fukaya, C. Matthieu, H. Yamochi, G. Saito, *J. Phys. IV France* **2004**, *114*, 143 – 145.
[17] P. Coppens, *Phys. Rev. Lett.* **1975**, *35*, 98 – 100.
[18] E. Espinosa, E. Molins, C. Lecomte, *Phys. Rev. B* **1997**, *56*, 1820 – 1833.
[19] F. Wudl, D. Nalewajek, J. M. Troup, M. W. Extine, *Science* **1983**, *222*, 415 – 417.
[20] E. Nishibori, M. Takata, K. Kato, M. Sakata, Y. Kubota, S. Aoyagi, Y. Kuroiwa, M. Yamakata, N. Ikeda, *Nucl. Instrum. Methods Phys. Res. Sect. A* **2001**, *467–468*, 1045 – 1048.
[21] M. Sakata, M. Sato, *Acta Crystallogr., Sect. A* **1990**, *46*, 263 – 270.
[22] H. M. Rietveld, *J. Appl. Crystallogr.* **1969**, *2*, 65 – 71.
[23] H. Tanaka, M. Takata, E. Nishibori, K. Kato, T. Iishi, M. Sakata, *J. Appl. Crystallogr.* **2002**, *35*, 282 – 286.
[24] S. Horiuchi, H. Yamochi, G. Saito, K. Sakaguchi, M. Kusunoki, *J. Am. Chem. Soc.* **1996**, *118*, 8604 – 8622.

  